Journal of the Korean Magnetic Resonance Society **2008**, *12*,1-13

Biotinoyl Domain of Human Acetyl-CoA Carboxylase: Structural Insights into the Carboxyl Transfer Mechanism

Chung-Kyung Lee[1†], Hae-Kap Cheong[1†], Kyoung-Seok Ryu[1], Jae Il Lee[2], Young Ho Jeon[1*] Chaejoon Cheong[1*]

[1]*The Magnetic Resonance Team, Korea Basic Science Institute, 804-1 Yangchung-Ri, Ochang, Chungbuk 363-883, Korea.*
[2]*The Division of Drug Discovery, CrystalGenomics, Inc., Asan Institute for Life Sciences, Pungna 2-dong, Songpa-gu, Seoul 138-736, Korea*
Received January 24, 2008

Abstract : Acetyl-CoA carboxylase (ACC) catalyzes the first step in fatty acid biosynthesis: the synthesis of malonyl-CoA from acetyl-CoA. As essential regulators of fatty acid biosynthesis and metabolism, ACCs are regarded as therapeutic targets for the treatment of metabolic diseases such as obesity. In ACC, the biotinoyl domain performs a critical function by transferring an activated carboxyl group from the biotin carboxylase domain to the carboxyl transferase domain, followed by carboxyl transfer to malonyl-CoA. Despite the intensive research on this enzyme, only the bacterial and yeast ACC structures are currently available. To explore the mechanism of ACC holoenzyme function, we determined the structure of the biotinoyl domain of human ACC2 and analyze its characteristics using NMR spectroscopy. The 3D structure of the hACC2 biotinoyl domain has a similar folding topology to the previously determined domains from *E. coli* and *P. Shermanii*, however, the 'thumb' structure is absent in the hACC2 biotinoyl domain. Observations of the NMR signals upon the biotinylation indicate that the biotin group of hACC2 does not affect the structure of the biotinoyl domain, while the biotin group for *E. coli* ACC interacts directly with the thumb residues that are not present in the hACC2 structure. These results imply that, in the *E. coli* ACC reaction, the biotin moiety carrying the carboxyl group from BC to CT can pause at the thumb of the BCCP domain. The human biotinoyl domain, however, lacks the thumb structure and does not have additional non-covalent interactions with the biotin moiety; thus, the flexible motion of the biotinylated lysine residue must underlie the "swinging arm" motion. This study provides insight into the mechanism of ACC holoenzyme function and supports the "swinging arm" model in human ACCs.

Keywords : Acetyl-CoA carboxylase, Biotinoyl domain, Biotinylation, NMR structure, BirA

* To whom correspondence should be addressed. E-mail : yhjeon@kbsi.re.kr, cheong@kbsi.re.kr
Chung Kyung Lee and Hae Kap Cheong contributed equally to this work.

INTRODUCTION

Acetyl-coenzyme A carboxylase (ACC) catalyzes the biotin-dependent carboxylation of acetyl-CoA to produce malonyl-CoA,[1] which participates both in the biosynthesis and metabolism of fatty acids and in the regulation of the mitochondrial shuttle system.[2-4] ACC also functions together with nucleoporins to control the nuclear accumulation of the small GTPase, Gsp1p.[5,6]

ACCs from prokaryotes have four separate polypeptide subunits,[7] whereas all four enzymatic activities are part of a single multifunctional polypeptide in eukaryotes. In human and other mammals, there are two ACC isoforms: ACC1 and ACC2.[8,9] ACC1 is predominantly expressed in lipogenic tissues such as liver and kidney, whereas ACC2 is preferentially expressed in skeletal muscle and heart. Differential expression of ACC1 and ACC2 has led to the hypothesis that ACC1 is involved in fatty acid biosynthesis and ACC2 in involved in fatty acid catabolism in muscle.[10]

The overall ACC reaction proceeds by a two-step mechanism. The first half-reaction is carried out by biotin carboxylase (BC) and involves the ATP-dependent carboxylation of biotin, in which bicarbonate serves as the CO_2 source. Carboxyl transferase (CT) catalyzes the second half-reaction in which the carboxyl group is transferred from biotin to acetyl-CoA to produce malonyl-CoA.[3,11]

The cofactor, biotin, must be attached to ACC to produce a functional enzyme. The biotin prosthetic group is attached to a specific lysine residue in the biotinoyl domain to yield the holo form, which swings between the BC and CT active sites.[5] In the "swinging arm" model, biotin is positioned at the end of a long, flexible lysine side chain and facilitates the translocation of CO_2 between BC and CT.[12] The biotinoyl domain of ACC participates in three heterologous protein-protein interactions. First, it serves as the substrate in the biotin ligation reaction catalyzed by a biotin protein ligase, which is known as BirA in prokaryotes and holocarboxylase synthetase in eukaryotes.[1] Second, the biotinylated form of this domain interacts with the BC subunit to incorporate CO_2 into the ureido group of the biotin ring system. Finally, the carboxylated biotin attached to this domain interacts with CT when the CO_2 moiety is transferred to acetyl-CoA to produce malonyl-CoA.

Extensive structural studies of the *E. coli* biotinoyl domain from biotin carboxyl carrier protein (BCCP) and, more recently the *Propionibacterium shermanii* 1.3S transcarboxylase subunit, have been reported.[13-15] Although some strands are one or two residues longer or shorter between the proteins [Fig. 1], the 1.3S transcarboxylase subunit structure of *P. shermanii* has a folding topology almost identical to that of the *E. coli* BCCP biotinoyl domain.[16]

ACCs are essential regulators of fatty acid biosynthesis and metabolism; thus, they are regarded as potential therapeutic targets for the treatment of metabolic diseases, including obesity. Research with ACC-deficient mice showed that these mice have elevated fatty acid oxidation and reduced body fat content and body weight, despite an increase in food consumption.[17] As such, clinical trials using ACC2 inhibitors are currently in progress.[18]

Despite the current interest in ACC, only a few bacterial protein structures have been reported, such as *E. coli* BCCP and *P. shermanii* 1.3S. Thus, there is no information on the structure of the ACC biotinoyl domain of higher eukaryotes, especially human. Here, we determined the solution structure of the biotinoyl domain of human ACC2 (hACC2) by NMR and investigated the structural characteristics.

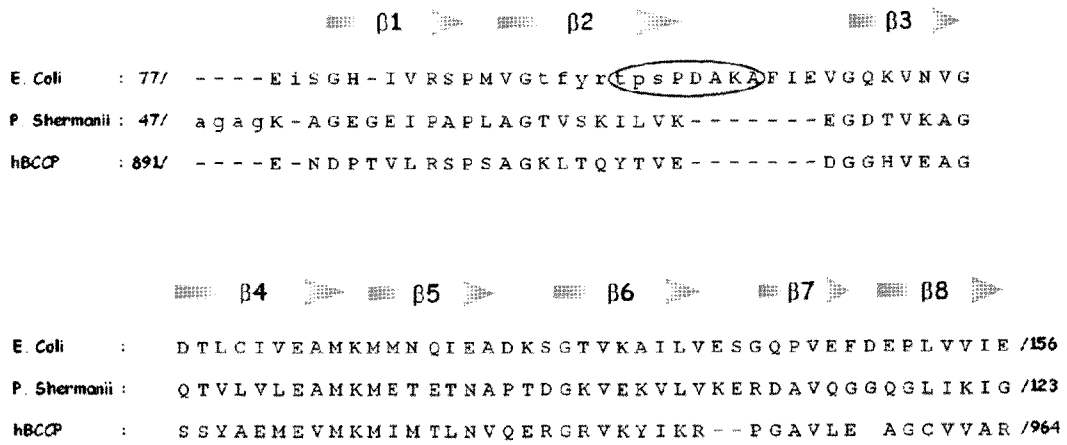

Fig. 1. Sequence alignment of biotinoyl domain with known structure. The secondary structure of the biotinoyl domain (based on NMR-driven structure) has been plotted on the top of the graph with the blue boxes. The numbers at the left and right of the sequences indicate the number of amino acids of each protein.

MATERIALS AND METHODS

Protein Expression and Purification

The DNA sequence for the biotinoyl domain (including residues 891-964 encoded by human *acc*2) was synthesized by PCR, and the product was digested with *BamH*I-*Xho*I and inserted into a pET-28a(+) vector (Novagen). After induction with 1 mM IPTG, the recombinant protein was expressed in *E. coli* (BL21λDE3 strain) (Invitrogen) for 14 h at 18°C. For uniform ^{15}N and ^{15}N, ^{13}C labeling, the cells were grown in M9 minimal medium[19] supplemented with $^{15}NH_4Cl$ with or without ^{13}C-labeled glucose (Cambridge Isotope). Soluble fraction of cell lysates were prepared by resuspending cells in lysis buffer (30 mM Tris·HCl, pH 8.0, 50 mM NaCl, 5 mM imidazole, 5% glycerol, 1 mM TCEP, 1 mM PMSF), followed by sonic disruption. After centrifugation, the supernatant was loaded into a Ni-chelating column (HiTrap FF 5, Amersham Bioscience), which has been equilibrated with lysis buffer excluded PMSF, and eluted with 300 mM imidazole. The fraction concentrated by ultrafiltration (Amicon) further purified by gel filtration (Superdex 75, Pharmacia) equilibrated with 50 mM HEPES, pH 7.3, 100 mM NaCl and 1 mM DTT.

Protein Biotinylation

The holo-biotinoyl domain was derived enzymatically from apo-protein by BirA-catalyzed biotin ligation. The *in vitro* biotinylation reaction contained the apo-protein (0.8 mM), BirA (Avidity) and biotin (500 μM), which was incubated for 3 days at 30°C with shaking at 200 rpm.[20] The mixture was then dialyzed against 50 mM HEPES, pH 7.3, and 1 mM DTT at 4°C to prevent aggregation due to biotin. The protein was concentrated by ultrafiltration (Amicon) and purified by gel filtration (Superdex 75, Pharmacia) equilibrated with 50 mM HEPES, pH 7.3, 100 mM NaCl and 1 mM DTT.

NMR Spectroscopy

NMR measurements were performed at 20°C on apo- and holo-protein samples in either 90% H_2O/10% D_2O or 100% D_2O, containing 50 mM HEPES, pH 7.3, and 1 mM DTT, on DRX500 and DRX800 spectrometers (Bruker). The protein preparation was concentrated to 0.2-1.0 mM for NMR experiments. For D_2O measurements, the protein was

lyophilized and redissolved in D_2O. All NMR spectra were processed with NMRPiPe[21] and analyzed with SPARKY 3.110.[22] Two-dimensional ^{1}H-^{15}N HSQC, ^{1}H-^{13}C HSQC, three-dimensional CBCA(CO)NH,[23] HNCACB,[24] and HNCO[25] NMR experiments were performed for the backbone assignment. Three-dimensional HBHA(CO)NH, C(CC-TOCSY-CO)N-NH,[26] H(CC-TOCSY-CO)N-NH, HCCH-TOCSY,[27] and TOCSY-N15-HSQC spectra were used for the side chain assignments. Distance restraints were derived from ^{15}N- or ^{13}C-resolved three-dimensional NOESY-HSQC spectra using mixing times of 150 ms. ^{15}N relaxation (T1, T2, and heteronuclear $\{^{1}H\}$-^{15}N NOE) was measured on ^{15}N-labeled apo- and holo-protein samples at 293 K with a 500-MHz 1H Larmor frequency. The ^{15}N longitudinal and transverse relaxation time constants, T1 and T2 respectively, were determined by acquiring a series of ^{1}H-^{15}N HSQC spectra with sensitivity enhancement.[28] For T1 measurements, the spectra were collected with relaxation delays of 10, 50, 100, 200, 300, 500, 800, and 1200 ms. For T2 measurements, data were acquired with delays of 20, 40, 60, 70, 90, 100, 140, and 170 ms. A total of 2048 complex data points with 256 complex increments were collected for the relaxation experiments. Steady-state ^{1}H-^{15}N NOEs were measured following the method described in Farrow *et al.*[28]

Structure Calculation

Restraints for the backbone dihedral angles φ and ψ were derived from chemical shifts using the program TALOS.[29] The automatic NOE assignment and structure calculations were performed using the CYANA program[30] and the 2580 NOE cross peaks (885 from ^{15}N-NOESY-HSQC and 1695 from ^{13}C-NOESY-HSQC). Ribbon and surface representations were prepared with CHIMERA[31] and GRASP,[32] respectively.

RESULTS AND DISCUSSION

Overall Structure and Shape

We have determined the solution structure of the hACC2 biotinoyl domain, residues 891-964, using heteronuclear NMR methods. The overall structure of the domain is globular and is formed by two very similar four-stranded sheets connected by small loops

and turns that surround a hydrophobic core in a sandwich-like manner [Fig. 2]. One β-sheet is comprised of β1, β3, β6, and β8, and the other is formed by β2, β4, β5, and β7; all strands are antiparallel. The eight β-strands are connected by four β-turns, one hairpin, and two short loops. The first loop connecting β1 and β2 and the second loop connecting β5 and β6 form a bridge between the two β-sheets at both ends. The biotin acceptor, Lys 929, is located in the hairpin between β4 and β5.

The tightly packed, buried hydrophobic core is formed between the two -sheets and is composed of hydrophobic residues [Fig. 2(C)]. In the calculated structure, side chains of these hydrophobic residues are very well-defined and presumably play an important role in stabilizing the β-sandwich structure..

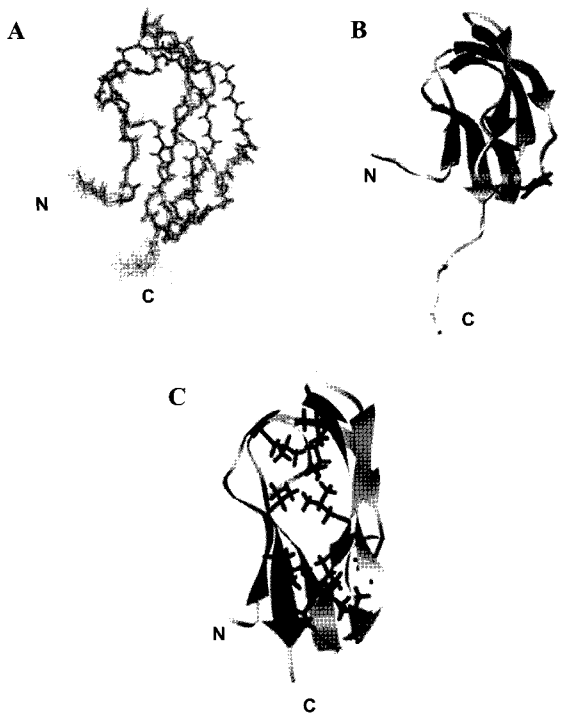

Fig. 2. The solution structure of the human ACC2 biotinoyl domain (residues 891-964). (A) Twenty structures of hACC2 biotinoyl domain are superimposed (residue range for r.m.s.d. calculation and matching is 895-960). The backbone region was well converged, and the r.m.s.d. was 0.31 Å. (B) Ribbon representation of the hACC2 biotinoyl domain. (C) Side chains of hydrophobic residues involved in forming the hydrophobic core.

Structural Comparison of Biotinoyl Domains

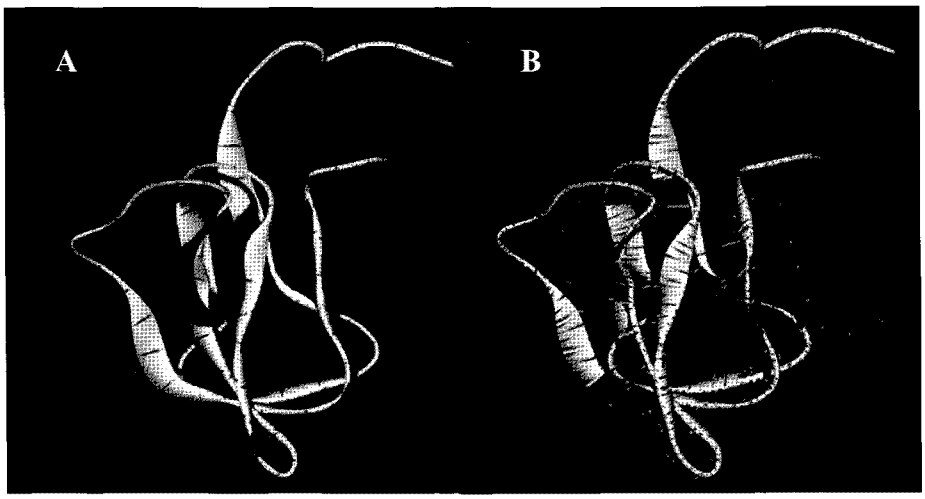

Fig. 3. Structural comparison of the biotinoyl domains. (A) *E. coli* biotinoyl domain is shown in red and the biotinoyl domain of human ACC2 is shown in yellow. (B) Ribbon diagram of the *P. shermanii* biotinoyl domain is shown in blue.

Comparison of the 3D structure of the hACC2 biotinoyl domain with that from *E. coli* and *P. Shermanii* suggests they have a similar folding topology with a root mean square deviation for the backbone atoms of 3.73 Å and 2.90 Å, respectively [Fig. 3]. In *E. coli* BCCP, two glutamic acid residues, Glu 119 and Glu147, interact with the basic residues in BirA of *E. coli*.[33] Several studies report that these negatively charged residues located near the biotinylation site are crucial for enzyme function.[33,34] Three-dimensional structural alignment suggests that Glu 119 and Glu 147 in *E. coli* BCCP are equivalent to Glu 926 and Glu 953 in the hACC2 biotinoyl domain, and Glu 86 and Gln 114 in *P. Shermanii* 1.3S, respectively.

Although the overall folding and positions of these two negatively charged residues are similar, the local structures near the biotinylation sites have notable differences between the human and bacterial biotinoyl domains. First, the MKM side chain geometry is represented in a clockwise orientation in *E. coli* and *P. shermanii*; however, this geometry is counter-clockwise in the human enzyme [Fig. 4]. Second, the "thumb" structure, which is composed of eight protruding residues between β2 and β3 in the *E. coli* domain, is not

present in the human domain. The thumb structure in *E. coli* is essential for the function of BCCP in the ACC reaction,[16] and deletion of the thumb results in failure of growth and fatty acid synthesis.[16] Because the thumb region in *E. coli* shows an interaction with the biotin moiety after biotinylation (see below),[36] the absence of the thumb structure in the hACC2 biotinoyl domain suggests that this domain may have a different feature of interaction with the biotin moiety. The absence of the thumb structure in hACC2 also implies that it has different physical properties from that of *E. coli* during the translocation of the biotin group between BC and CT..

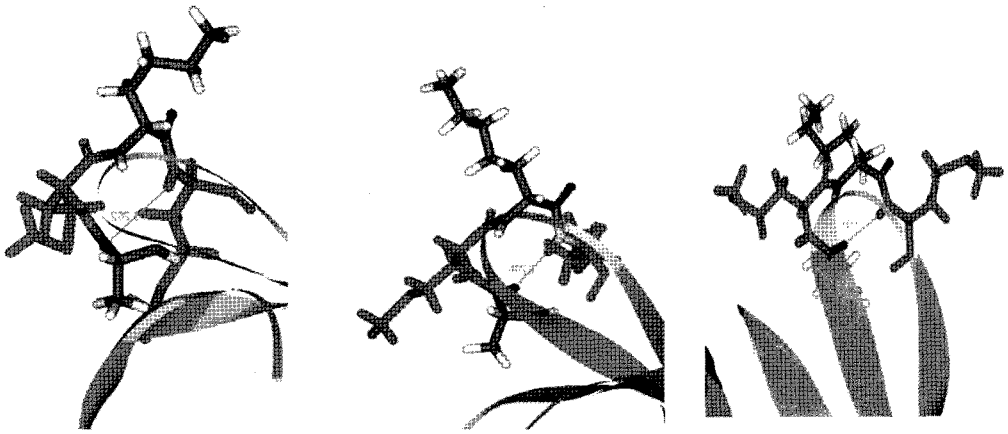

Fig. 4. Clockwise orientation of MKM side chain in *E. coli* and *P. shermanii* and counter-clockwise in hACC2.

Biotinylation of hACC2

We performed the biotinylation reaction with the *E. coli* BCCP and human ACC2 biotinoyl domains using *E. coli* biotin protein ligase, BirA. Biotinylation of *E. coli* BCCP showed significant chemical shift changes for the residues around the biotinylation site, Cys 116-Gln 126, and the thumb region, Gly 89-Phe 102 [Fig. 5(B)].[37] However, biotinylation of the human domain showed only small chemical shift changes, specifically localized to residues near Lys 929, where the biotin prosthetic group is covalently attached [Fig. 5(A)]. Thus, the biotin group in the holo form of hACC2 does not have additional interactions with

the biotinoyl domain except the covalent bonding with Lys 929, distinct from the case of *E. coli* ACC where the biotin group shows direct interaction with the thumb residues.

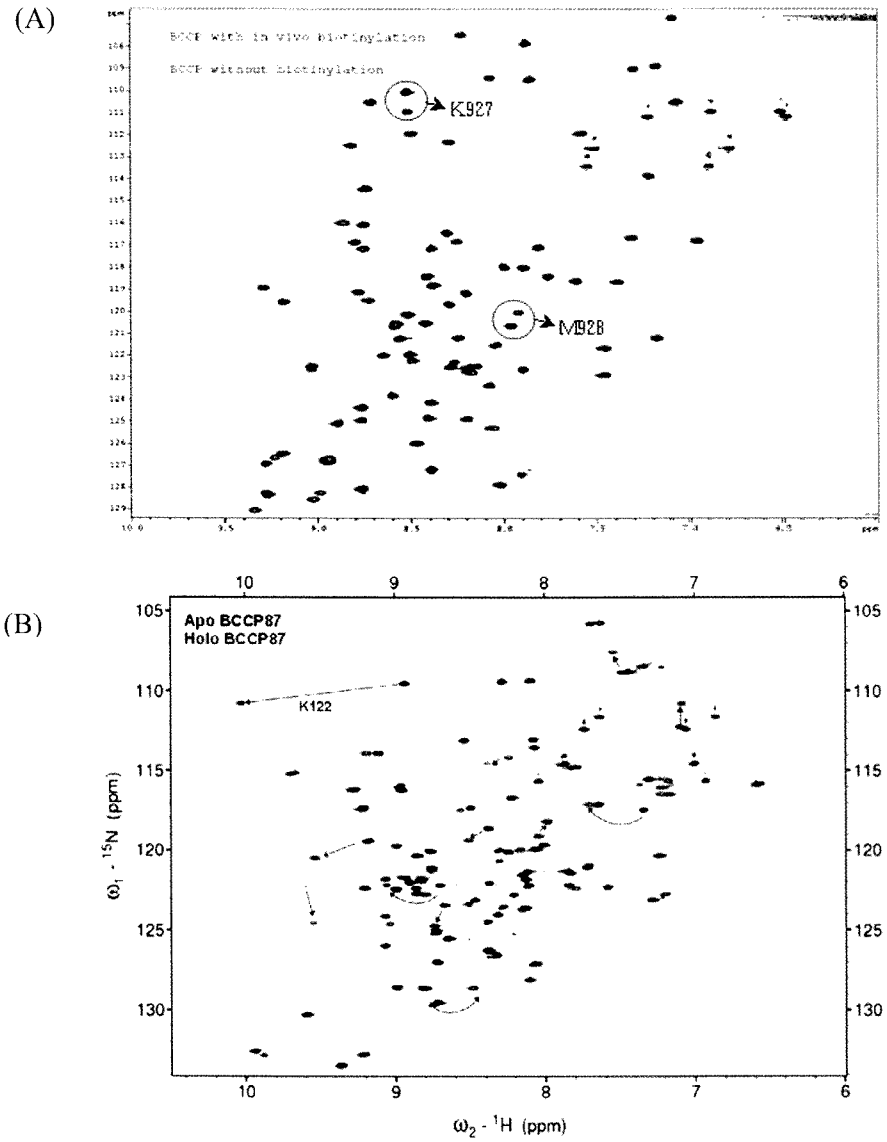

Fig. 5. Comparison of the apo- and holo-biotinoyl domains. (A) Overlays of the two-dimensional ^{1}H-^{15}N HSQC spectra for ^{15}N-labeled apo- and holo-human ACC2 biotinoyl domain. Cross peaks for the apo and holo proteins are shown in black and red, respectively. (B) Overlays of two-dimensional ^{1}H-^{15}N HSQC spectra for the apo- and holo- *E. coli* biotinoyl domain (BCCP87).

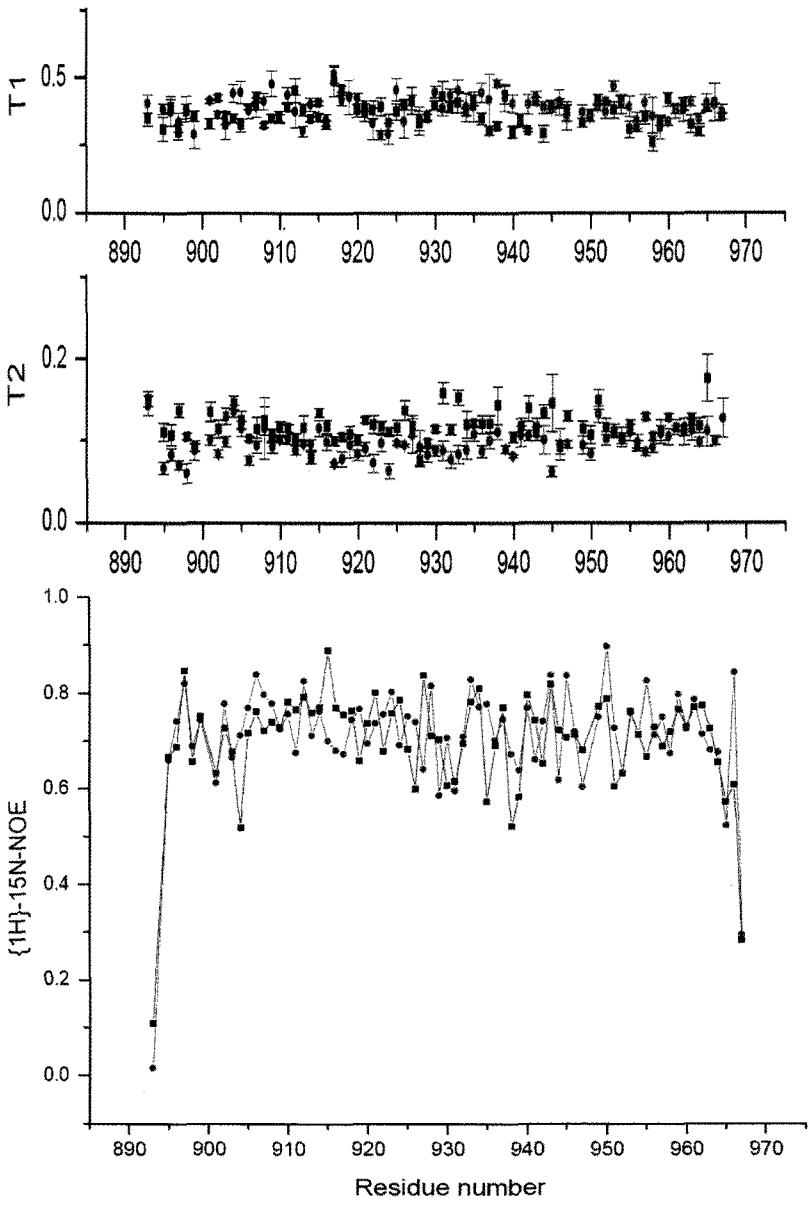

Fig. 6. Summary of NMR relaxation data of the biotinoyl domain from apo- and holo-hACC2. The ^{15}N T1, T2 and steady-state ^{1}H-^{15}N NOE values are represented with the residue numbers. Apo protein is indicated by red symbols, and holo protein is shown in green.

Structural comparison between the apo and holo hACC2 biotinoyl domains using the backbone H_N-Cα coupling constant measurements showed no remarkable differences. The backbone dynamics analysis using the ^{15}N T_1, T_2 and steady-state ^1H-^{15}N NOE measurements showed that the apo and holo biotinoyl domains have similar mobility [Fig. 6]. Although the apo biotinoyl domain shows slightly lower T1 and higher T2 values for several residues when compared with the holo form, these differences are not significant.

These findings suggest different structural features for biotinylated ACCs among different species. In *E. coli*, the biotin moiety, covalently bound to the lysine side chain of the biotinoyl domain, has additional non-covalent interactions with the thumb motif, including hydrogen bonding between the backbone and γ oxygen atoms of Thr 94 and the N1' and O2' atoms of the ureido ring in the biotin moiety, respectively.[16,38] In the *E. coli* ACC reaction, the biotin moiety carrying the carboxyl group from BC to CT can pause at the thumb of the BCCP domain. The human biotinoyl domain, however, lacks the thumb structure and does not have additional non-covalent interactions with the biotin moiety; thus, the flexible motion of the biotinylated lysine residue must underlie the "swinging arm" motion. Moreover, the hACC2 biotinoyl domain along with the BC and CT domains are in a common polypeptide. These findings thus suggest that the hACC2 biotinoyl domain indeed functions as a "swinging arm"

In summary, we have described the solution structure of the biotinoyl domain of hACC2 and analyzed its structure and interaction with biotin ligase upon biotinylation. Three-dimensional structural comparisons among the mammalian and bacterial biotinoyl domains showed notable differences including the geometry of the 'Met-Lys-Met' side chain, and the absence of 'thumb' structure in the hACC2 biotinoyl domain. We also suggest the critical differences in the interaction of biotin group with the biotinoyl domain and the carboxyl transfer mechanism between bacterial and human biotinoyl domain of ACC. This study provides insight into the essential role of biotinylation in fatty acid metabolism, and supports the "swinging arm" model whereby the biotinoyl domain plays role in the ACC enzymatic reaction.

Acknowledgement

We thank Dr. John Cronan, Jr. and Dr. Anne Chapman-Smith for the gift of plasmid

pTM53. This work was supported by funds from the 21C Frontier Functional Proteomics Project (Y.H.J), and the Bio-MR Research Program (Y.H.J., Korea Basic Science Institute) of the Korean Ministry of Science & Technology.

REFERENCES

1. P. A. Diana, S. V. Sergio, L. D. R. Alfonso, *Arch Med Res.*, **33**, 439-447 (2002)
2. J. D. McGarry, N. F. Brown, *Eur. J. Biochem.*, **244**, 1-14 (1997)
3. J. E. Cronan, G. L. Waldrop, *Prog Lipid Res.*, **41**, 407-435 (2002)
4. Y. Sasaki, Y. Nagano, *Biosci Biotechnol Biochem.*, **68**, 1175-1184 (2004)
5. L. Tong, *Cell Mol Life Sci.*, **62**, 1784-1803 (2005)
6. H. Gao, N. Sumanaweera, S. M. Bailer, U. Stochaj, *J. Biol. Chem.*, **278**, 25331-25340 (2003)
7. C. R. Eunjoo, E. C. John, *J. Biol. Chem.*, **33**, 30806-30812 (2003)
8. L. Abu-Elheiga, A. Jayakumar, A. Baldini, S. S. Chirala, S. J. Wakil, *Proc Natl Acad Sci USA.*, **92**, 4011-4015 (1995)
9. J. Widmer, K. S. Fassihi, S. C. Schlichter, K. S. Wheeler, B. E. Crute, N. King, N. Nutil-McMenemy, W. W. Noll, S. Daniel, J. Ha, K. H. Kim, L. A. Witters, *J. Biochem.*, **316**, 915-922 (1995)
10. L. Abu-Elheiga, D. B. Almarza-Ortega, A. Baldini, S. J. Wakil, *J. Biol. Chem.*, **272**, 10669-10677 (1997)
11. J. R. Knowles, *Ann Rev Biochem.*, **58**, 195-221 (1989)
12. S. J. Wakil, J. K. Stoops, V. C. Joshi, *Ann Rev Biochem.*, **52**, 537-579 (1983)
13. F. K. Athappilly, W. A. Hendrickson, *Structure*, **3**, 1407-1419 (1995)
14. Y. Xiang, W. Dong, S. J. Cylburn, F. S. Michael, B. Dorothy, *Biochemistry*, **36**, 15089-15100 (1997)
15. D. V. Reddy, B. C. Shenoy, P. R. Carey, F. D. Sonnichsen, *Biochemistry*, **39**, 2509-2516 (2000)
16. E. C. John, *J. Biol. Chem.*, **276**, 37355-37364 (2001)

17. L. Abu-Elheiga, M. M. Martin, A. H. Khaled, J. W. Salih, *Science*, **291**, 2613-2616 (2001)
18. T. Zhang, R. F. Clark, T. M. Hansen, Z. Xin, G. Liu, X. Wang, R. Wang, H. S. Camp, H. S. Beutel, H. Sham, G. Y. Gui, *San Francisco: ACS Meeting*, 232th (2006)
19. A. Contreras, S. Molin, J. L. Ramos, *Appl Environ Microbiol*, **57**, 1504-1508 (1991)
20. P. J. Schatz , *Biotechnology.*, **11**, 1138-1143 (1993)
21. F. Delaglio, S. Grzesiek, G. Vuister, G. Zhu, J. Pfeifer, A. Bax, *J. Biomol. NMR*, **6**, 277-293 (1995)
22. T. D. Goddard, D. G. Kneller, *SPARKY 3. University of California, San Francisco.*
23. S. B. Grzesiek, *J. Am. Chem. Soc.*, **114**, 6291-6293 (1992)
24. M. M. Wittekind, *J. Magn. Reson.*, **B101**, 201-205 (1993)
25. M. Ikura, L. E. Kay, A. Bax, *Biochemistry*, **29**, 4659-4667 (1990)
26. S. B. Grzesiek, J. Anglister, A. Bax, *J. Magn. Reson.*, **B101**, 114-119 (1993)
27. A. Bax, G. M. Clore, P. C. Driscoll, A. M. Gronenborn, M. Ikura, L. E. Kay, *J. Magn. Reson.*, **87**, 620-627 (1990)
28. N. A. Farrow, R. Muhandiram, A. U. Singer, S. M. Pascal, C. M. Kay, G. Gish, S. E. Shoelson, T. Pawson, I. D. Forman-Kay, L. E. Kay, *Biochemistry*, **33**, 5984-6003 (1994)
29. G. Cornilescu, F. Delaglio, A. Bax, *J. Biomol. NMR*, **13**, 289-302 (1999)
30. T. Herrmann, P. Güntert, K. Wüthrich, *J. Mol. Biol.*, **319**, 209-227 (2002)
31. C. C. Huang, G. S. Couch, E. F. Pettersen, T. E. Ferrin, *Pacific Symp Biocompu.*, **1**, 724 (1996)
32. A. Nicholls, K. A. Sharp, B. Honig, *Proteins Struct Funct Gene.*, **11**, 281-296(1991)
33. C. S. Anne, D. M. Terrence, w. Fiona, E. C. John, C. W. John, *Protein Sci.*, **10**, 2608-2617 (2001)
34. C. S. Anne, W. M. Timothy, C. W. John, John EC. *J. Biol. Chem.*, **274**, 1449-1457 (1999)
35. B. L. Sibanda, J. M. Thornton, *Natur.*, **316**, 170-174 (1985)
36. S. Jose, C. S. Anne, E. C. John, *J. Biol. Chem.*, **277**, 21604-21609 (2002)
37. Y. Xiang, S. Cylburn, F. S. Michael, B. Dorothy, *Protein Sci.*, **8**, 307-317 (1999)
38. L. R. Emma, S. Ningcheng, J. H. Mark, B. William, C. S. Anne, C. W. John, M. Tim, E. C. John, N. P. Richard, *Biochemistry*, **38**, 5045-5053 (1999)